https://doi.org/10.22226/2410-3535-2023-1-14-19

Assessing residual stresses in the surface layer of the ZK60 alloy after an exposure to corrosion solution

E. D. Merson[†,1], V. A. Poluyanov[1], A. V. Polunin[1], P. N. Myagkikh[1],
D. L. Merson[1], A. Yu. Vinogradov[2]

[†]Mersoned@gmail.com

[1]Institute of Advanced Technologies, Togliatti State University, Togliatti, 445667, Russia
[2]Department of Mechanical and Industrial Engineering, Norwegian University of Science and Technology — NTNU, Trondheim, N-7491, Norway

Magnesium alloys preliminary immersed in a corrosion solution suffer from embrittlement, referred to as pre-exposure stress corrosion cracking (PESCC). It was suggested that PESCC can be attributed to the corrosion product film-induced stress (CPFIS), which is known to be responsible for SCC in many alloys. However, the internal stress associated with the formation of the corrosion products (CP) layer on Mg alloys have not been investigated as yet. Thus, in the present study, the internal residual stresses of the first and second kinds were assessed in the alloy ZK60 exposed to the corrosion solution, using the deflection of the thin plate and by the X-ray diffraction technique, respectively. It is found that the deposition of CP on the surface of the alloy ZK60 creates the compressive internal stresses of both kinds — I and II. The macro residual stress of the kind I in the thin plate is found to be not exceeding 3 MPa, while the micro residual stress of the second type in the surface layer of 20 – 30 μm can be as high as 290 MPa and cause plastic deformation of the bare metal with the internal stress which cannot be relieved by the removal of CP.

Keywords: magnesium alloys, pre-exposure stress corrosion cracking, internal stress, corrosion products-film induced stress.

1. Introduction

The combined action of corrosive media and mechanical stresses (both internal and external) is known to cause stress corrosion cracking (SCC) of many structural alloys, including those based on magnesium [1]. Magnesium is a chemically active element, and as such it is prone to easy corrosion. Under slow-strain rate tensile testing in various environments, including saline and distilled water, Mg alloys commonly experience a remarkable drop of mechanical properties coupled with the concomitant change in the fracture mode from the ductile to brittle one [2]. Furthermore, the characteristic features of SCC can also appear during mechanical testing in relatively inert environments, e. g., in air, if the Mg alloy has been preliminary soaked into a corrosive solution (even for a fairly short time) [3 – 5]. The specific conditions inducing the pronounced embrittlement effect, referred to as pre-exposure SCC (PESCC), have been considered suggestive of hydrogen being the root cause of SCC [4 – 6]. The electrochemical corrosion of Mg is intrinsically accompanied by the cathodic reduction of hydrogen. It was supposed that a part of this hydrogen can be absorbed by Mg in the form of mobile atoms, which, under the applied stress, could diffuse quickly through the material and promote brittle cracking according to the commonly known hydrogen embrittlement mechanisms [7]. However, recent experimental findings have strongly suggested that it is the layer of corrosion products (CP) deposited on the surface of the alloy during pre-exposure, which plays a decisive role in the mechanism of PESCC, and not hydrogen dissolved in the metal matrix [8 –10]. In particular, it was found that PESCC of the ZK60 and AZ31 alloys could be completely eliminated by the removal of CP from the specimens pre-exposed to NaCl-based corrosive media [8 –10]. Furthermore, the existence of the relationship between the amount of CP on the surface and the extent of PESSC in ZK60 has been reported [9]. A few possible scenarios of possible influence of CP on the mechanism of PESCC have been considered and discussed. For instance, the CP layer can serve as a "container" for the embrittling agents, such as hydrogen or retained corrosive solution. These agents, in turn, assist the nucleation of brittle cracks at the side surface, and facilitate their further propagation into the bulk metal [8 –11]. The presence of the corrosion solution in the CP layer, as well as its interaction with the crack surface, was witnessed by the crust of CP covering the peripheral area of the fracture surface [8 –10]. It was established that the region covered by CP on the fracture surface is formed exactly during tensile testing, because its size was reduced with increasing strain rate [8]. Besides, no cracks with CP inside were observed in the pre-exposed specimens before tensile testing [8]. Furthermore, the evolution of extra hydrogen from the pre-exposed ZK60 samples after extraction from the corrosion solution was detected. This was considered as the additional

evidence for the corrosion reaction occurring at the interface between the CP layer and bare metal [11]. The extremely high concentration of hydrogen was found in the CP layer, however, the firm evidence for its role in PESCC is still to be gained [10]. Finally, it is known that, due to volumetric incompatibility between CP and the base metal, the CP layer deposited on the metal surface can cause the high internal stress in the matrix, referred to as corrosion products film induced stress (CPFIS) [12–17]. This stress is usually tensile, and is maximum is reached at the interface between the CP layer and the metallic substrate [12]. The CPFIS was concluded to be the primary cause of SCC in a number of alloys, including Ti- [17], Cu- [12,15] and Fe-based ones [13,14]. Nevertheless, the data on internal stress associated with deposition of the CP layer in Mg alloys has not been reported as yet. In view of the high significance of this issue for understanding the nature of SCC and PESCC, the present study is aimed at the assessing of the CPFIS in ZK60 alloy pre-exposed to the NaCl-based corrosion solution doped by potassium dichromate.

2. Experimental

2.1. Materials and samples

The commercial hot-extruded alloy ZK60 with the chemical composition provided in Table 1 and the aqueous corrosion solution of 4 wt.% NaCl + 4 wt.% $K_2Cr_2O_7$ were used for all the experiments in the present study. It was thoroughly documented in our previous reports that, after pre-exposure during 1.5 h to the same corrosion solution, this alloy suffers from substantial embrittlement, which is almost fully eliminated by removal of CP [8–10]. To assess the internal stresses, which can be associated with the CP layer deposited on the samples' surface, two different sets of experiments have been performed: (1) the experiments with a thin plate to assess the magnitude and sign of the residual macro stress of the first kind; (2) the X-ray diffraction (XRD) profile analysis — to assess the magnitude of the internal micro stresses of the second kind. Using the electric-discharge machine, the thin rectangular plates of $48 \times 5 \times 0.19 \pm 0.01$ mm dimensions were cut along the extrusion direction for the first set of experiments, and the disks of 20 mm diameter and 0.8 mm thickness were cut across the extrusion direction for the XRD analysis. All samples were subjected to vacuum annealing at 250°C for 2 hours before exposure to the corrosion solution.

2.2. Macro stress of the first kind (type I)

The magnitude and the sign of macro residual stresses of the first kind were assessed by the deflection of the thin plate exposed to the corrosion solution. The plates with one side varnished were vertically immersed in the corrosion solution for 30 or 90 minutes. As the plate was extracted from the corrosive medium, it was carefully cleaned with ethanol and dried with compressed air inducing no pressure sufficiently high to deflect the plate. To measure the deflection of the plate, one end of the plate was fixed by a weight on the flat horizontal surface as it is schematically illustrated in Fig. 1. The height distance between the opposite end of the plate and the base surface was measured using the confocal laser scanning microscope (CLSM) Lext OLS4000 (Olympus). Five height measurements along the width of the plate were made and the magnitude of the deflection, Δ, was calculated as their average value. In this way, the deflection was measured (i) before the exposure to corrosive medium, Δ_1, (ii) after the exposure to the corrosion solution followed by the removal of the varnish, Δ_2, and (iii) after the subsequent removal of the CP layer, Δ_3. The removal of the varnish and the CP-layer was conducted by immersion of the corroded plate respectively in the ultrasonic bath with acetone and in the standard C.5.4 (20% CrO_3 + 1% $AgNO_3$) aqueous solution for 1 min in accordance with GOST R 9.907. The type I residual macro stress, σ_I, giving rise to the measured plate deflection before and after removal of corrosion products was estimated using the Eq. (1):

$$\sigma_I = \frac{\Delta h E}{l^2} \qquad (1)$$

where Δ and h are the deflection and the thickness of the plate at specific conditions, $l = 47$ mm is the length of the freely bended plate, see Fig. 1, and $E = 42.8$ GPa is the Young's modulus of pure Mg.

The deflections before and after exposure to the corrosion solution as well as after removal of corrosion products were calculated as: $\Delta_{ref} = \Delta_1 - h_{ref}$, $\Delta_c = \Delta_2 - \Delta_1 - h_c$ and $\Delta_{cp} = \Delta_3 - \Delta_1 - h_{cp}$, where h_{ref}, h_c and h_{cp} are the thicknesses of the plate before exposure, after exposure and after removal of CP, respectively. Since the decrease of l was negligible during corrosion, the same initial value was used for all calculations.

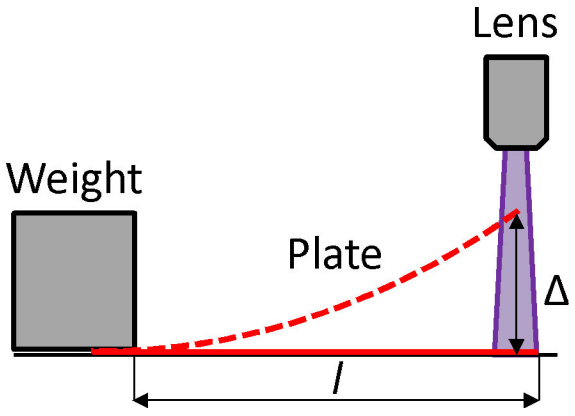

Fig. 1. (Color online) The schematics of the experimental setup for the measurement of the deflection of the corroded plate.

Table 1. Chemical composition of the alloy ZK60 (in wt.%).

Mg	Al	Zn	Ca	Zr	Fe	Cu	Mn	Ce	Nd	Si
Balance	0.002	5.417	0.0004	0.471	0.001	0.002	0.005	0.002	0.003	0.003

2.3. Micro-stress of the second kind (type II)

To assess the internal microscopic stresses of the second kind, the disc samples were immersed in the corrosion solution at room temperature for different times ranging from 5 to 360 minutes. After extraction from the corrosion solution, the samples were cleaned with ethanol and dried with compressed air. From several samples exposed to the corrosion solution for 90 minutes, the CP were removed in accordance with the standard procedure used in the experiments with varnished thin plate described above. The XRD analysis was started within 5 minutes after the extraction of the sample from corrosive medium. The reference samples, which did not interact with the corrosion solution were analyzed as well.

The XRD analysis of the samples for both the volumetric analysis of the phase composition and assessment of the stress state/residual micro-stresses was performed in the Bragg-Brentano geometry, using the Maxima XRD-7000S (Shimadzu) diffractometer (CuK_α radiation, long fine focus (LFF) X-ray tube, tube current 30 – 40 mA, voltage 30 – 40 kV, scanning speed 0.25° min^{-1}, step 0.01°) in the 2θ angles range of 10 – 100 deg. To improve the signal-to-noise ratio, the curved graphite monochromator was used on the diffracted-beam side. The assessment of residual micro stresses (micro strains) in a thin surface layer of the alpha-matrix (α-Mg) of the alloy was performed in the grazing incidence diffraction/thin film (GIXRD) mode with a constant irradiation angle of 5° with the same power parameters "on the tube" and scanning speed/step. In this mode, the estimated depth of the analyzed surface layer was about 20 – 30 μm. The crystalline phases were identified using the Shimadzu PDF2 database. The full-profile analysis of diffractograms was performed by the Le Bail and Rietveld methods in the Jana software. The Chebyshev's polynomial was used to simulate the background, and the Voigt/Pseudo-Voight profile function was adopted to describe the reflections of the crystalline phases. The asymmetry of the reflections (correction by divergence), the deviations of the lattice parameters from the reference ones, and the shift of the gravity centers of the reflections of the identified phases have been evaluated during the analysis. The quality of the computational models was achieved in terms of GOF (goodness of fit) and wRp (weighted profile factor) no worse than 3% and 8%, respectively. The sizes of crystallites by Scherrer (Dcrist) and the relative residual strains ε (micro stresses) according to the Stokes-Wilson method for the phases of the oxide layers were determined, assuming the Scherrer constant $K=1$. The recalculation of the residual Stokes-Wilson micro strains of the alpha matrix of the alloy to the micro stresses was done through the elasticity modulus of pure magnesium.

3. Results

3.1. Visual examination

It is found that during exposure of the plate and disc samples to the corrosion solution their surface is quickly covered by a dark film of CP, Fig. 2. Even after five minutes of exposure, the dark spots were already abundantly present on the surface, Fig. 2 b, while after 30 minutes, the surface was completely covered by the solid film of CP, Fig. 2 d. It was also ensured that the varnished surface of the samples exhibited no signs of corrosion damage or CP. The microscopic morphological features of CP which are formed on ZK60 alloy in the same corrosion solution to that used in the present paper as well as their chemical composition can be found elsewhere [8, 9, 11].

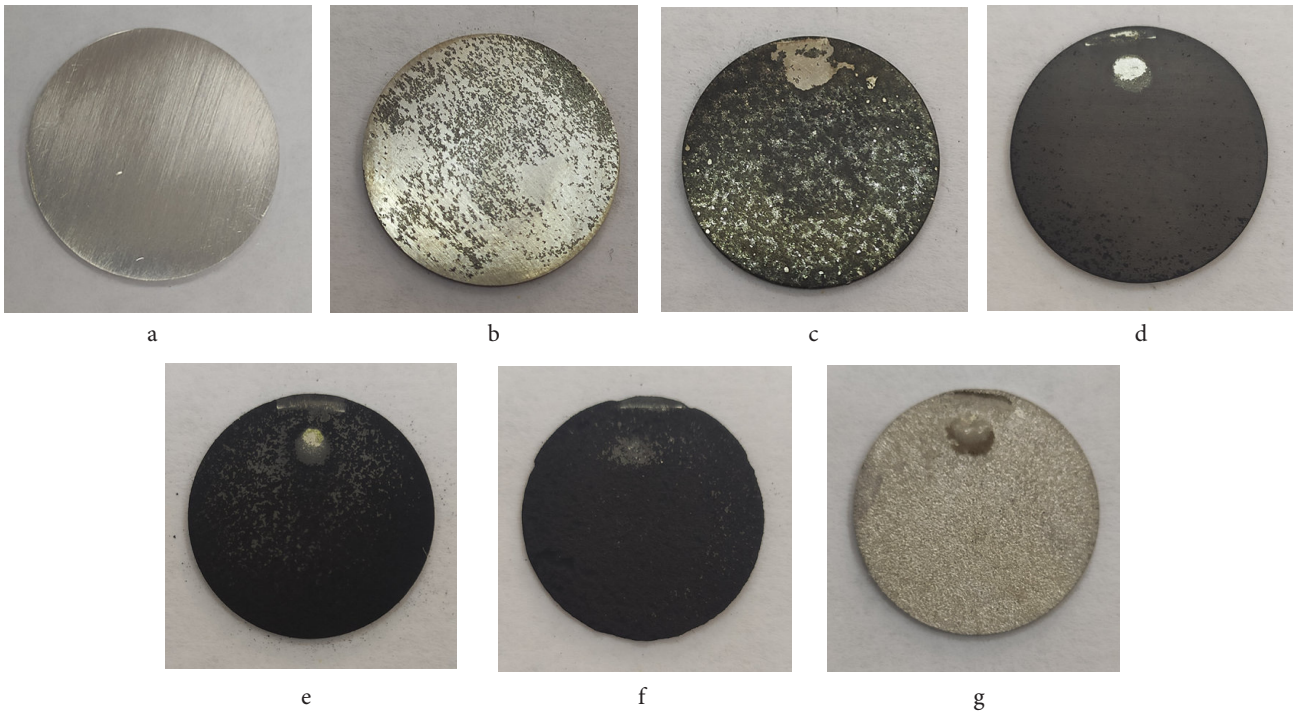

Fig. 2. (Color online) The disc samples of the alloy ZK60 in the reference state (a) and after exposure to corrosion solution for 5 min (b), 15 min (c), 30 min (d), 90 min (e, g), 360 min (f). The sample in (g) is after removal of corrosion products.

3.2. XRD analysis

The XRD spectra obtained in the GIXRD scanning mode from the reference disc samples, which were not interacted with the corrosion solution, exhibit peaks corresponding to the α-Mg phase and the secondary phase particles of $MgZn_2$, see profile #1 in Fig. 3. According to the volumetric phase composition analysis, the concentration of $MgZn_2$ phase is 1.1%.

The analysis of the XRD spectra obtained in the same scanning mode from the disc samples, which were exposed to the corrosive medium for different times, showed that the intensity of the peaks corresponding to α-Mg and $MgZn_2$ phases is substantially reduced due to the formation of the CP on the surface, see spectra #2 – 5 in Fig. 3. However, no peaks associated with the components of CP are found on the XRD spectra regardless of the amount of CP on the surface. This fact, as well as the pronounced halo in the low-angle domain on the XRD spectra for corroded samples, suggests that the CP are mostly amorphous.

From the analysis of the residual micro-strains in the reference samples by the XRD spectra obtained in the GIXRD scanning mode, the type II micro-stresses are found to have the value of 99 ± 3 MPa. It follows from Fig. 4 that the exposure of the samples to the corrosion solution leads to a remarkable increase in internal micro-stresses as well as to a decrease in the size of the coherent scattering regions (CSR) in the surface layer of the metal. Within the first 5 minutes of exposure, the increase in the micro-stress is negligible. However, the decrease of the CSR is already notable even after this short period of exposure. The dramatically steep increase of micro-stresses up to the maximum value of 290 MPa occurs in the time interval from 5 to 30 minutes of exposure. The increase of the micro-stress is accompanied by the decrease of the CSR from 38 to 15 nm. During the next 60 minutes of exposure, the micro-stresses slightly decrease down to 277 MPa, while the CSR increases up to 16 nm. During the further exposure up to 4.5 h, both the micro-stress and the CSR value remain

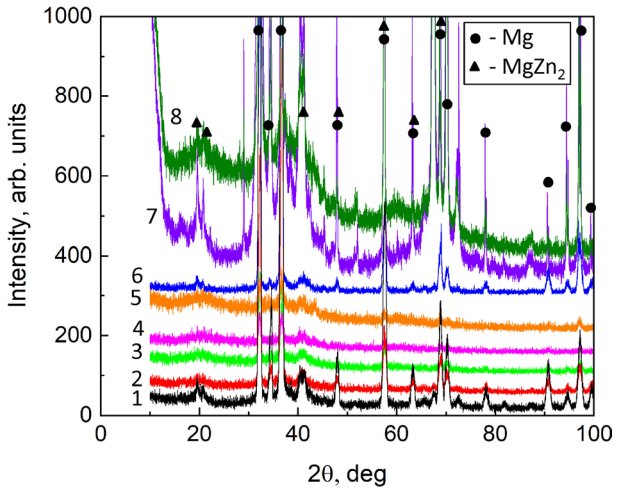

Fig. 3. (Color online) The XRD spectra obtained in the GIXRD (1–6) and regular (7, 8) scanning modes from the disc samples of the alloy ZK60 in the reference state (1, 7) and after exposure to the corrosion solution for 15 min (2), 30 min (3), 90 min (4, 6, 8), 360 min (5). The spectrum (6) is for the sample after removal of corrosion products.

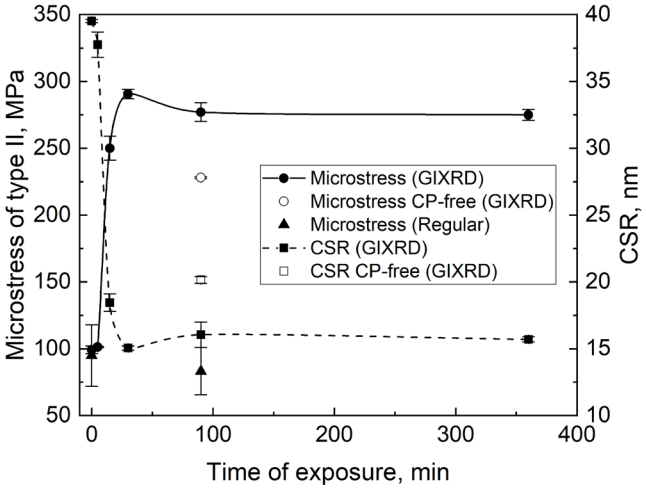

Fig. 4. The effect of time of exposure to the corrosion solution on the internal stress of the second kind and the coherent scattering region (CSR) in ZK60.

constant. After removal of CP from the samples, which were exposed to the corrosion solution for 90 minutes, the internal stress decreases from 277 to 230 MPa. Nevertheless, this stress is still more than twice the micro-stress in the reference samples. Since CP were completely removed from the plates and no microstructural transformations are expected to occur during the corrosion, the residual increase in the micro-stress is suggested to be due to plastic deformation. Apparently, the stress associated with the formation of CP is high enough to trigger plastic deformation in the surface layer of the sample. The magnitude of the micro-stress calculated from the XRD spectra supports this suggestion: this magnitude appreciably exceeds the yield stress (220 MPa) of the alloy ZK60 used in the present study but are slightly lower than its ultimate tensile strength (300 MPa).

The results described above were calculated from the XRD spectra obtained in the GIXRD mode, thus, they relate to the surface layer of about 20 – 30 μm depth. In contrast, the XRD spectra obtained in the regular mode characterize the bulk of the sample having the 0.8 mm thickness. Thus, for comparison, the sample exposed to the corrosion solution for 90 minutes was scanned in the regular mode, see profile #8 in Fig. 3. The analysis of the obtained XRD spectra showed that the micro-stress corresponding to the corroded sample was of the same order as for the reference ones. The difference between the magnitude of micro-stresses in the reference samples determined from the XRD spectra which were obtained in the regular and GIXRD modes was negligible. Thereby, the micro-stress induced by CP are concentrated in the relatively narrow surface layer, the exact depth of which, however, is unknown.

3.3. The experiments with thin plates

The experiments showed that during exposure to the corrosion solution, the thin plates of the alloy ZK60, the one side of which was preliminarily varnished, deflect towards the side covered with CP, Fig. 5. Considering that before immersion in the corrosion solution the plates exhibited negligible deflection, one has to conclude that there is a

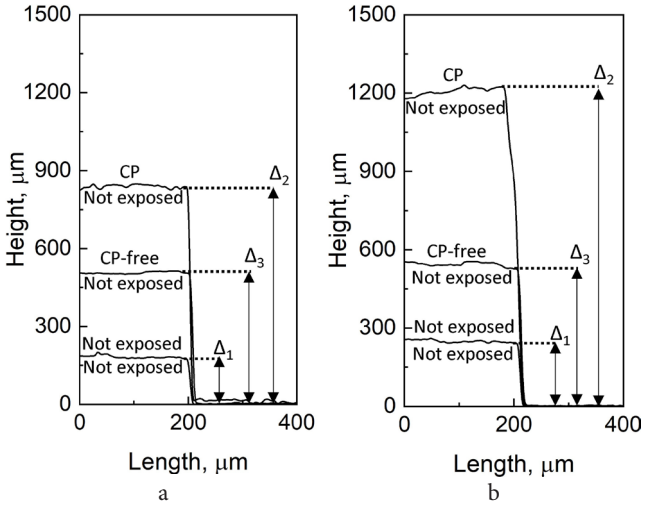

Fig. 5. The height profiles illustrating the deflection of the thin plates of the alloy ZK60 before exposure to corrosion solution, Δ_1, after 30 (a) and 90 min (b) of exposure, Δ_2, and after removal of corrosion products, Δ_3. The profiles are obtained with the use of CLSM from the edge of the plates as is schematically shown in Fig. 1.

compression stress evolved during the exposure process and induced by the CP layer deposited on the surface. It is established that the deflection of the corroded plates, which was measured after removal of the varnish, increases with time of exposure to the corrosion solution. Magnitudes of the macro-stress, σ_1^I, calculated from the measured deflections are found to be 1.7±0.7 and 2.5±0.1 MPa for the samples pre-exposed to the corrosion solution for 30 and 90 minutes, respectively (Table 2). The macro-stress was calculated in account for the reduction of the plates thickness due to corrosion, which is found to be of the order of 0.01±0.005 mm and 0.035±0.005 mm for the samples exposed to the corrosive solution for 30 and 90 minutes, respectively. After removal of CP, the plates remain bended towards the corroded side, albeit the magnitude of deflection decreases. The macro-stress corresponding to the residual deflection of the samples after removal of CP, σ_2^I, is found to not exceed 0.7±0.4 and 0.4±0.2 MPa after exposure to the corrosion solution for 30 and 90 minutes, respectively. The observed residual deflection of the corroded plate corroborates well with the results of the XRD analysis indicating that the plastic deformation occurred within the surface layer during corrosion. However, the depth of this plastically deformed surface layer should be quite small because on the scale of the whole sample the macro-stress is relatively low. This conclusion agrees perfectly with the XRD data too. Thereby, the compression macro-stress induced by the deposition of the CP layer results in the bending strain of the plate; this strain consists of two components: (1) the elastic one, which is directly associated with presence of the CP layer on the surface, and (2) the plastic one, which is associated with plastic deformation of the thin surface layer beneath the CP layer. The macro-stress associated with elastic component of strain relieves after removal of CP as is indicated by the reduction of deflection of the plate as well as by a decrease of the micro-stress of type II in the surface layer. The magnitude of the change in deflection after removal of CP can be used for assessing the macro-stress associated directly with CP being deposited on the surface of the plate, σ_3^I. This stress is found to be about 1.1±0.1 and 2.1±0.3 MPa for the samples, which were exposed to the corrosion solution for 30 and 90 minutes, respectively.

Table 2. The effect of time of exposure to the corrosion solution on the internal stress of type I in the 0.2 mm thick plates of ZK60 alloy with one side varnished right after extraction from corrosive medium, σ_1^I, and after removal of corrosion products, σ_2^I. σ_3^I is the stress directly associated with the presence of corrosion products layer on the surface.

Time of exposure, min	σ_1^I, MPa	σ_2^I, MPa	σ_3^I, MPa
30	1.7±0.7	0.7±0.4	1.1±0.1
90	2.5±0.1	0.4±0.2	2.1±0.3

4. Discussion

The obtained results show that, in contrast to many other alloys in which the CPFIS is tensile [12,16,17], the ZK60 alloy experiences compressive macro stress due to the deposition of the CP layer in the 4% NaCl + 4% $K_2Cr_2O_7$ corrosion solution. Unlike the tensile one, the compressive CPFIS does not favor the nucleation of cracks in the surface layer, and, thus, can hardly be responsible for SCC. Furthermore, the magnitude of this stress on the macro scale is found to be too low to cause a significant change in the mechanical properties of the bulk specimens — the specimens with the geometry and dimensions, which are commonly used for assessing SCC and PESCC. Thus, relieving of CPFIS associated with the CP layer deposited on the surface of the ZK60 alloy under the investigated conditions cannot explain the complete elimination of PESCC after removal of the CP layer from the side surface of the specimens, which was reported recently in [8–10]. Nevertheless, it is shown that the micro-stress induced by the surface film of CP in the thin surface layer of the alloy can be large enough to cause plastic deformation. It was shown in the recent studies that the corrosion solution can retain within the CP layer even after extraction of the specimen from corrosive media [8,11]. During the subsequent tensile testing, this corrosion solution sealed within the CP layer, interacts with the bare metal in the wake of the propagating cracks as is evidenced by the crust of CP abundantly present on the fracture surface of the pre-exposed specimens [8]. Assuming that the formation of CP can induce extremely large stress capable of plastic deformation of the base metal, one may suggest that this CPFIS can probably significantly facilitate the propagation of the brittle crack, because its blunting in the plastically deformed metal should be limited, regardless of whether the compressive or tensile stress was responsible for plastic deformation. Thus, when the corrosion solution continuously contacts the bare metal inside the propagating crack either in pre-exposed specimens tensile tested in air or in the specimens stretched right in the corrosion solution the CPFIS associated with formation of CP at the crack tip can be at least partially responsible for PESCC and SCC of Mg alloys. However, a further study is required to reveal the exact role of CPFIS in the mechanism of these phenomena.

5. Conclusions

1. The formation of corrosion products (CP) on the surface of the ZK60 alloy exposed to the 4% NaCl + 4% $K_2Cr_2O_7$ corrosion solution induces compressive internal stresses of type I and II in the base metal.

2. The macro-stress of type I in the 0.2 mm thick plate of ZK60 alloy covered with CP is found to be of the order of 1.7 and 2.5 MPa after 30 and 90 minutes of exposure, respectively.

3. The micro-stress of type II in the surface layer of 20 – 30 μm thickness is found to be maximum and equal to 290 MPa after 30 minutes of exposure.

4. The removal of CP from the surface of the ZK60 alloy results in a decrease of the corrosion products film induced stress (CPFIS) of type I and II, however, the residual compressive stresses of both types presumably associated with plastic deformation of the base metal remain even after removal of the CP layer.

5. The elimination of pre-exposure stress corrosion cracking of the alloy ZK60 due to removal of CP cannot be explained solely by relieving of internal stress, however, CPFIS, which arises in the bare metal contacting with corrosion solution at the tip of the propagating crack can likely facilitate PESCC and SCC.

Acknowledgements. Financial support from the Russian Science Foundation through grant No. 18-19-00592 is gratefully appreciated.

References

1. A. Atrens, W. Dietzel, P. Bala Srinivasan, N. Winzer, M. Bobby Kannan. Stress corrosion cracking (SCC) of magnesium alloys. In: Stress Corros. Crack. Elsevier (2011) pp. 341– 380. Crossref
2. N. Winzer, A. Atrens, G. Song, E. Ghali, W. Dietzel, K. U. Kainer, et al. Adv. Eng. Mater. 7, 659 (2005). Crossref
3. D. G. Chakrapani, E. N. Pugh. Metall. Trans. A. 7, 173 (1976). Crossref
4. S. Jafari, R. K. S. Raman, C. H. J. Davies. Eng. Fract. Mech. 201, 47 (2018). Crossref
5. D. B. Prabhu, J. Nampoothiri, V. Elakkiya, R. Narmadha, R. Selvakumar, R. Sivasubramanian, et al. Mater. Sci. Eng. C. 106, 110164 (2020). Crossref
6. M. Kappes, M. Iannuzzi, R. M. Carranza. Corrosion. 70, 667 (2014). Crossref
7. M. Kappes, M. Iannuzzi, R. M. Carranza. J. Electrochem. Soc. 160, C168 (2013). Crossref
8. E. Merson, V. Poluyanov, P. Myagkikh, D. Merson, A. Vinogradov. Mater. Sci. Eng. A. 830, 142304 (2022). Crossref
9. E. Merson, V. Poluyanov, P. Myagkikh, D. Merson, A. Vinogradov. Acta Mater. 205, 116570 (2021). Crossref
10. E. Merson, V. Poluyanov, P. Myagkikh, D. Merson, A. Vinogradov. Mater. Sci. Eng. A. 806, 140876 (2021). Crossref
11. E. Merson, V. Poluyanov, P. Myagkikh, D. Merson, A. Vinogradov. Lett. Mater. 12 (1), 76 (2022). Crossref
12. X. S. Du, Y. J. Su, C. Zhang, J. X. Li, L. J. Qiao, W. Y. Chu, et al. Corros. Sci. 69, 302 (2013). Crossref
13. X. S. Du, Y. J. Su, J. X. Li, L. J. Qiao, W. Y. Chu. Corros. Sci. 65, 278 (2012). Crossref
14. M. Asawa, A. Devasenapathi, M. Fujisawa. Mater. Sci. Eng. A. 366, 292 (2004). Crossref
15. X. Guo, K. Gao, L. Qiao, W. Chu. Metall. Mater. Trans. A. 32, 1309 (2001). Crossref
16. W. Wang, Z. Zhang, X. Ren, Y. Guan, Y. Su. Sci. Rep. 5, 1 (2015). Crossref
17. X. Z. Guo, K. W. Gao, W. Y. Chu, L. J. Qiao. Mater. Sci. Eng. A. 346, 1 (2003). Crossref